Cancer Letters 443 (2019) 179–188

Contents lists available at ScienceDirect

Cancer Letters

journal homepage: www.elsevier.com/locate/canlet

Original Articles

MicroRNA-371a-3p promotes progression of gastric cancer by targeting TOB1

Hai Guo[a,*], Fuzhi Ji[a], Xiaofeng Zhao[a], Xiaozhong Yang[b], Jingdong He[a], Lingling Huang[a], Yuanyuan Zhang[c]

[a] Department of Oncology, The Affiliated Huaian No.1 People's Hospital of Nanjing Medical University, China
[b] Department of Digestive, The Affiliated Huaian No.1 People's Hospital of Nanjing Medical University, China
[c] Department of Clinical Laboratory, The Affiliated Huaian No.1 People's Hospital of Nanjing Medical University, China

ARTICLE INFO

Keywords:
Gastric cancer
miR-371a-3p
TOB1
Prognosis-associated
Metastasis
Oncogenic

ABSTRACT

An integrated study was conducted to identify the potential prognosis biomarker of the gastric cancer. The study analyzed the expression level of microRNAs (miRNAs) and clinical follow-up information of gastric cancer patients. miR-371-3p was determined as a promising biomarker for the prognosis of GCs among the 74 dysregulated miRNAs examined. The qRT-PCR analysis of the expression of miR-371-3p in 121 GC tumors confirmed its overexpression and correlation with aggravation of the GC patients. The *in vitro* functional assays demonstrated that overexpression of miR-371-3p promoted proliferation, colony formation, migration and invasion of the GC cells, whereas miR-371-3p depletion led to the opposite. The findings were further confirmed by the *in vivo* knockdown of miR-371-3p experiment: the depletion of miR-371-3p inhibited tumor growth and metastasis. Based on the results of the bioinformatics analysis and bioassays, TOB1 was found to be the direct target of miR-371-3p, functioning as a tumor suppressor in GC cells. TOB1 was prerequisite for miR-371-3p to promote cell proliferation and migration. In conclusion, the results suggest that miR-371-3p is a potential prognosis biomarker and therapeutic target for GC.

1. Introduction

Gastric cancer (GC) is the fifth most frequently occurring cancer worldwide, with 951,000 new cases each year, accounting for 6.8% of all cancers [1], and the second leading cause of cancer-related deaths. Surgical resection is the most effective strategy for GC treatment, with a five-year survival rate of 5–20% for patients with advanced GC [2]. The mechanisms of initiation and progression remain poorly understood due to its heterogeneity. Therefore, studies on dissecting molecular mechanisms underlying the development of GC to provide effective and novel biomarkers for diagnosis and prognosis prediction are urgently needed.

MicroRNAs (miRNAs), with an average length of 18–22 nucleotides, are endogenous small single-stranded non-coding RNA molecules, causing mRNA cleavage and subsequent degradation by binding to the complementary 3' untranslated region (UTR) of the mRNA [3]. miRNAs have been found to participate in regulating cell proliferation, differentiation, metabolism and apoptosis [4]. Although a number of miRNAs have been reported to participate in the development and progression of GC, including miR-34 [5], miR-199 [6], 125a-5p [7] and miR-148a [8], the pathogenic mechanism has not been fully understood yet. Thus, more functional evidence and investigation of clinical significance are needed to elucidate the pivotal roles of miRNAs in GC.

The Transducer of ERBB2, 1 (*TOB1*) encodes a TOB/B cell translocation gene (BTG) family protein, which has been established as an anti-proliferative protein with an *N*-terminal TOB/BTG domain, containing two short elements, Box-A and Box-B [9]. Previous studies have reported that TOB1 functions as a tumor suppressor that inhibits cancer cell migration and proliferation, and enhances radio-sensitivity through various signaling pathways [10–12]. More importantly, down-regulation of TOB1 was observed in various types of cancer, such as breast [12] and stomach [10]. Emerging evidence has established TOB1 regulation by dysregulated microRNA (miRNA) network in other types of cancer [13]. However, in GC this has not been investigated.

In the present study, we performed an integrated analysis to identify GC-associated dysregulated miRNAs critical for GC development and progression. miR-371a-3p was found to be up-regulated in GC tumor tissues and high level of miR-371a-3p was correlated with shorter overall survival and disease-free survival in GC patients. Findings from *in vitro* and *in vivo* functional assay indicated that miR-371a-3p plays a

* Corresponding author. Department of oncology, The Affiliated Huaian No.1 People's Hospital of Nanjing Medical University, Nanjing, 223300, PR China.
E-mail address: HaiGuozxc@163.com (H. Guo).

https://doi.org/10.1016/j.canlet.2018.11.021
Received 20 June 2018; Received in revised form 19 November 2018; Accepted 21 November 2018

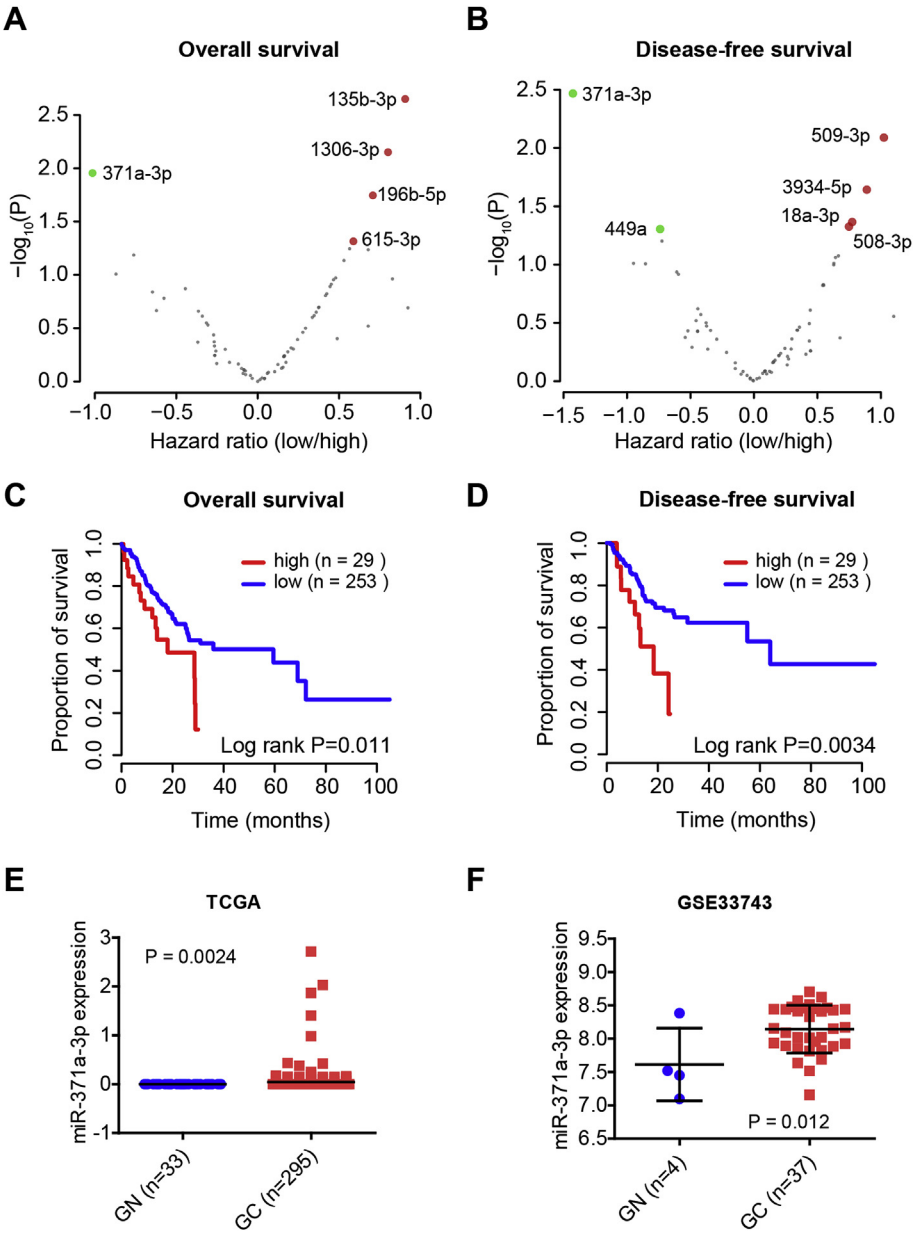

Fig. 1. Integrated analysis of GC miRome identifies miR-371a-3p. (**A–B**) Volcano plot of overall survival (**A**) and disease-free survival (**B**) analyses of dysregulated miRNAs in GCs. The P value and hazards ratio were calculated by log-rank test and Cox proportional hazards regression analysis, respectively. The GC patients were grouped by the average expression value of each dysregulated miRNAs. Red spots indicate high level of miRNA, predicting better survival, while green spots indicate high level of miRNA, which predicts poor survival. The miRNA expression data and clinical information were obtained from the TCGA project. (**C–D**) Kaplan-Meier curves indicate that poor overall survival (**C**) and disease-free survival (**D**) in GC patients is positively associated with miR-371a-3p expression level. The GC patients were stratified into "high" and "low" groups by the average expression levels of miR-371a-3p. (**E–F**) The expression levels of miR-371a-3p in TCGA dataset (**E**) and GSE33743 (**F**) dataset. Student's *t* tests were performed. Data are presented as mean ± SD (*$P < 0.05$, ** $P < 0.01$, ***$P < 0.001$). (For interpretation of the references to colour in this figure legend, the reader is referred to the Web version of this article.)

tumor-promoting role in enhancing GC cell growth and metastasis. TOB1 was found to be directly targeted by miR-371a-3p, in which TOB1 was down-regulated by miR-371a-3p in GCs. Most importantly, our results showed that TOB1 plays a tumor-suppressive role in GC cells, and it is required for the miR-371a-3p's oncogenic activities in GC cells. These findings provide advancements in the ongoing effort to understand GC tumorigenesis, and provide a potential strategy for the treatment of GC patients by inhibiting miR-371a-3p.

2. Methods

2.1. Cell lines and GC tissues

Human GC cell lines AGS and MKN-45 were maintained in RPMI-1640 medium (Gibco, USA) supplemented with 10% fetal bovine serum (Gibco, USA) in a humidified atmosphere containing 5% carbon dioxide at 37 °C. A total of 121 primary GC tumors, 10 of which with matched metastatic tumors and non-tumor tissues were obtained from the Affiliated Huaian No.1 People's Hospital of Nanjing Medical University from 2014 to 2016. All samples were histologically classified as GC by two pathologists. The use of human samples was approved by the Affiliated Huaian No.1 People's Hospital of Nanjing Medical University. All TCGA data was obtained from http://cancergenome.nih.gov/.

2.2. RNA extraction and real-time quantitative RT-PCR (qRT-PCR)

Total RNA was isolated from the cells and GC tissues by using the RNAiso Plus Kit (Takara, Japan) and cDNA was synthesized using the PrimeScript RT reagent Kit (Takara, Japan). qRT-PCR was conducted using the iQ5 (Bio-Rad, USA) according to the manufacturer's protocols. For miRNAs, reverse transcription was performed using a TaqMan microRNA RT Kit (Applied Biosystems, Germany). Then, the product was pre-amplified, and the level of miR-371a-3p was measured by qRT-PCR using a TaqMan miRNA assay (assay 002124, Applied Biosystems, Germany). $2^{-\Delta\Delta CT}$ method was used to determine the relative expression levels.

2.3. miRNA mimics, inhibitor and transfection

Human miR-371a-3p mimics, control mimics, miR-371a-3p

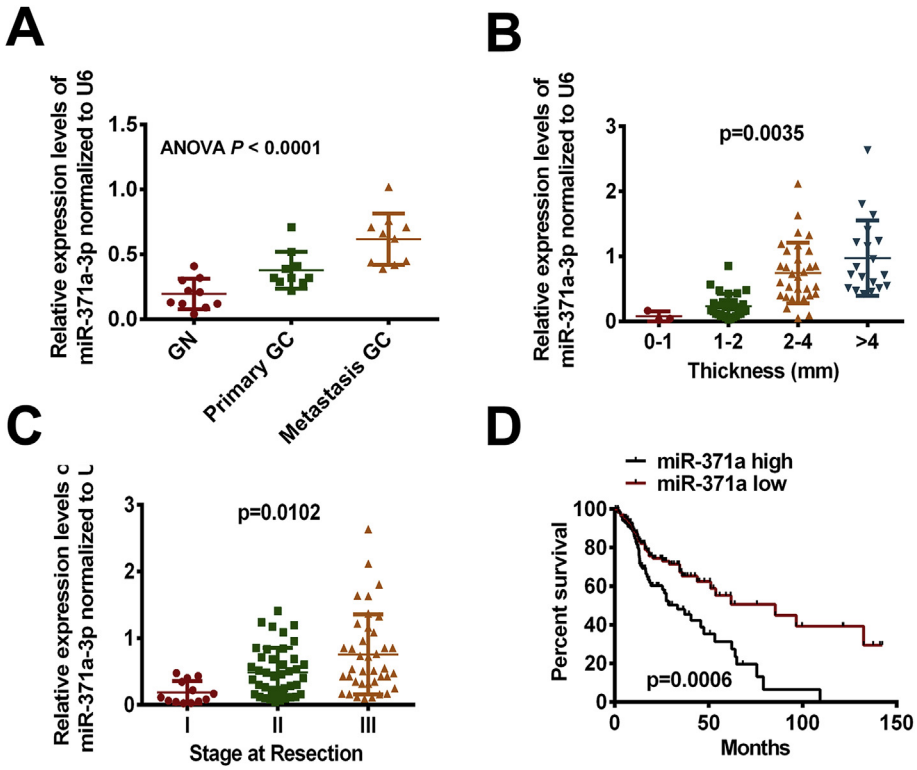

Fig. 2. Clinical significance of miR-371a-3p in GCs. (**A**) Relative expression levels of miR-371a-3p in a collection of matched non-tumor tissues, primary GC tumors and metastatic tumors (n = 10). The expression level of miR-371a-3p was assessed by qRT-PCR and normalized to U6. P value was calculated by ANOVA test. (**B**) Relative expression levels of miR-371a-3p in primary GC tumors (n = 121) grouped by the thickness of gastric wall, and (C) grouped by tumor stage at resection. P value was calculated by ANOVA test. (**D**) Kaplan-Meier curves indicate a positive correlation between poor overall survival and miR-371a-3p expression level in our GC cohort. P value was calculated by log-rank test. Data are presented as mean ± SD (*$P < 0.05$, **$P < 0.01$, ***$P < 0.001$).

inhibitor, control inhibitor, miR-371a-3p antagomir, control antagomir and shRNAs targeting TOB1 were generated by RiboBio Co. Ltd. (Guangzhou, China). Cells were transiently transfected using Lipofectamine 2000 (Invitrogen, USA) with a final concentration of 50 nM qRT-PCR was used to assess the transfection efficiency.

2.4. CCK-8 assay

Cell proliferation was assessed using the CCK-8 kit (Dojindo, Japan). Briefly, 4×10^3 cells per well were seeded in a 96-well plate. At different time points (time points: day 0, day 1, day 2, day 3, day 4 and day 5) 24 h after the transient transfection, cells were incubated with 12 μL of CCK-8 for 4 h, and the density was measured with a microplate reader (Biotek, USA) at 490 nm.

2.5. Cell migration and invasion assay

Cell migration and invasion were assessed by transwell chambers (diameter: 6.5 mm, membrane pore size: 8 μm; Corning, USA). Membranes coated with 1 mg/mL Matrigel (BD Biosciences, USA) were used for invasion assays, whereas for migration assays, Matrigel was not used. 5×10^4 cells were resuspended in 200 μL serum-free medium and added to the upper chamber. Then, 600 μL of DMEM containing 20% FBS was added to the lower chamber. Following incubation at 37 °C for 24 h, the non-migrating or non-invading cells were removed with cotton swabs. Finally, invading cells on the lower side of the filter were fixed with 4% paraformaldehyde at room temperature for 30 min and stained with 1% crystal violet.

2.6. Protein extraction and western blotting

Total protein was extracted from cells using RIPA lysis buffer (Beyotime, China) according to the manufacturer's instructions. Protein concentration was quantified using the Bradford kit (Beyotime, China) according to the manufacturer's protocols. Equal amount of protein samples were separated using 10% SDS-PAGE gel and transferred to a PVDF membrane, followed by 5% fat-free milk in TBST blocking and incubation with primary antibodies: anti-TOB1, (1:1,000, sc-133095, Santa Cruz, USA) and anti-GAPDH (1:1,000, sc-420485, Santa Cruz, USA) at 4 °C overnight. The membranes were then washed 3 times in TBST and incubated with anti-mouse horseradish peroxidase-conjugated secondary antibody for 1 h (1:500, sc-2005, Santa Cruz, USA). The protein bands were detected by the enhanced chemiluminescence method (ECL, Millipore) and visualized using a multifunctional protein imaging system (Cell biosciences, USA).

2.7. Luciferase activity assay

The miR-371a-3p binding site in TOB1 3′ UTR was predicted using the TargetScan 6.0. The wild-type vector (pmiR-RB-REPORT-h-TOB1 WT) and mutant vector (MUT) of the TOB1 3′ UTR were constructed by RiBoBio (Guangzhou, China). HEK293T cells were seeded in 24-well plates (1×10^5 cells/well) in triplicate. Twenty-four hours later, 5 nM of miR-371a-3p mimics or control mimics and 400 ng of pmiR-RBREPORT-h-TOB1 vector (WT or MUT) were co-transfected using Lipofectamine 2000 (Invitrogen, USA) according to the manufacturer's protocols. Luciferase activity was measured 36 h after transfection by the Dual-Glo luciferase assay system (Promega, USA). HRluc was the fluorescence reporter and hluc was used as the internal reference.

2.8. In vivo mouse studies

For *in vivo* tumor xenograft study, 2×10^6 MKN-45 cells were transfected with negative control or miR-371a-3p antagomir. Cells were then resuspended in 0.2 mL of sterile saline and xenografted subcutaneously into each flank of the immune-deficient nude mice (6-weeks old Balb/c nude mice, n = 6 for each group). The tumor sizes were measured weekly for a period of five weeks. The volume of xenograft tumors was calculated as follows: length × width^2 × 1/2. Mice were sacrificed and the tumors were excised from the body and subjected tohematoxylin-eosin staining, and immunohistochemistry

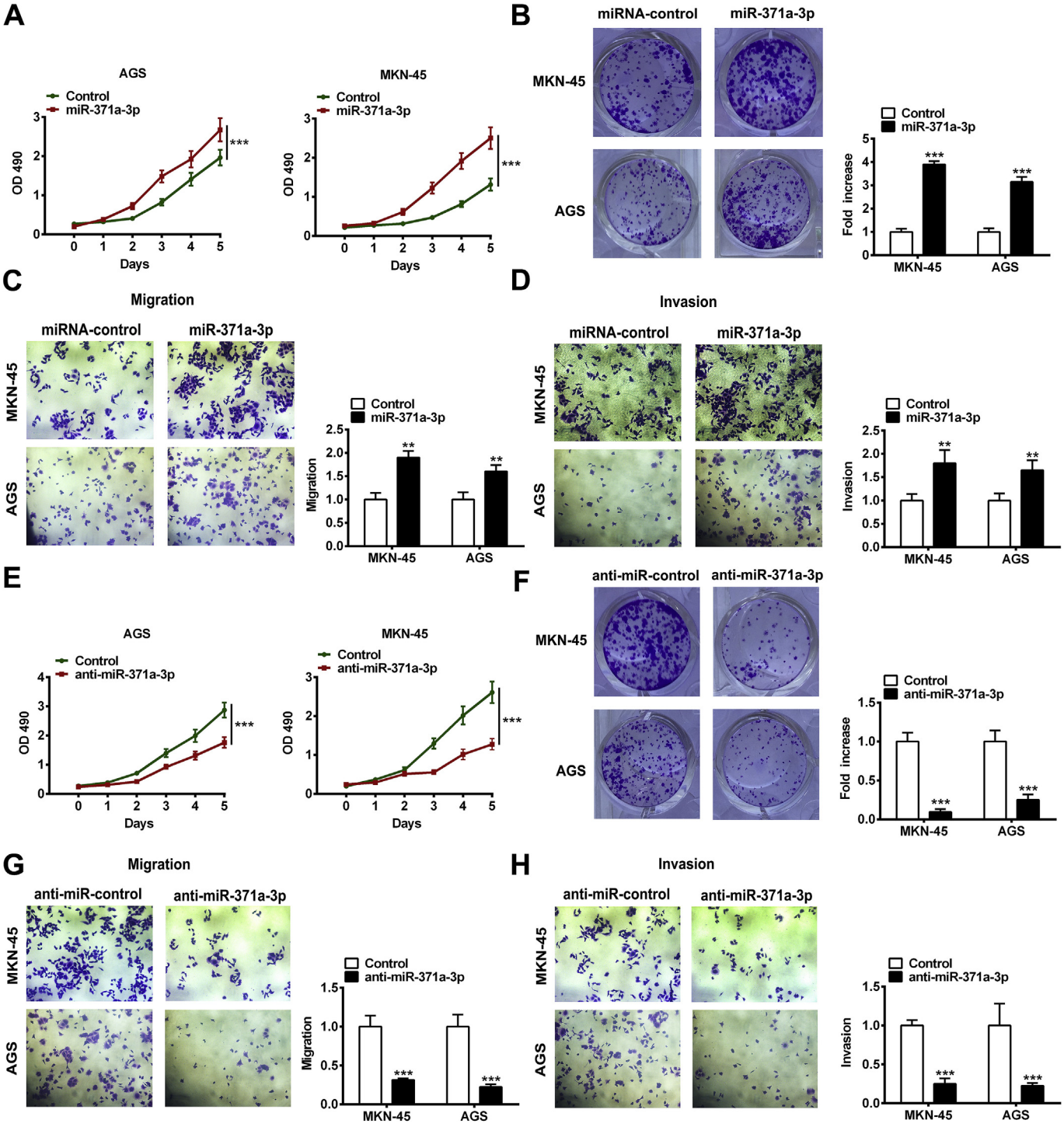

Fig. 3. miR-371a-3p promotes GC cell proliferation, migration and invasion.(**A-D**) Effects of miR-371a-3p overexpression on (A–B) cell proliferation by CCK8 assay and colony-forming assay, respectively, (C) cell migration (transwell assay), and (D) cell invasion (transwell assay) in AGS and MKN-45 cells. (E–H) Effects of inhibitor-induced miR-371a-3p knockdown on (E–F) cell proliferation by CCK8 assay and colony-forming assay, respectively, (G) cell migration (transwell assay), and (H) cell invasion (transwell assay) in AGS and MKN-45 cells. In CCK assays, cell proliferation was tested every 24 h. Student's *t* tests were performed. Data are presented as mean ± SD (**P* < 0.05, ** *P* < 0.01, ****P* < 0.001).

staining with TOB1 and Ki-67 antibodies.

For *in vivo* bioluminescence study, 2×10^6 luciferase-tagged MKN-45 cells transfected with negative control or miR-371a-3p antagomir were injected into the tail vein of immunodeficient nude mice (6-weeks old Balb/c nude mice, n = 6 for each group). The lung metastases were monitored by bioluminescent imaging (BLI) for four weeks. The *in vivo* BLI was carried out with an IVIS Spectrum Imaging System (Caliper) comprised of a highly sensitive, cooled CCD camera mounted in a light tight specimen box. Images and measurements of bioluminescent signals were acquired and analyzed with the Living Image software (Caliper). Mice were sacrificed, the lungs were excised from the body and subjected to hematoxylin-eosin staining, and immunohistochemistry staining with TOB1 and CD34 antibodies.

An animal protocol was approved by the Animal Care and Use

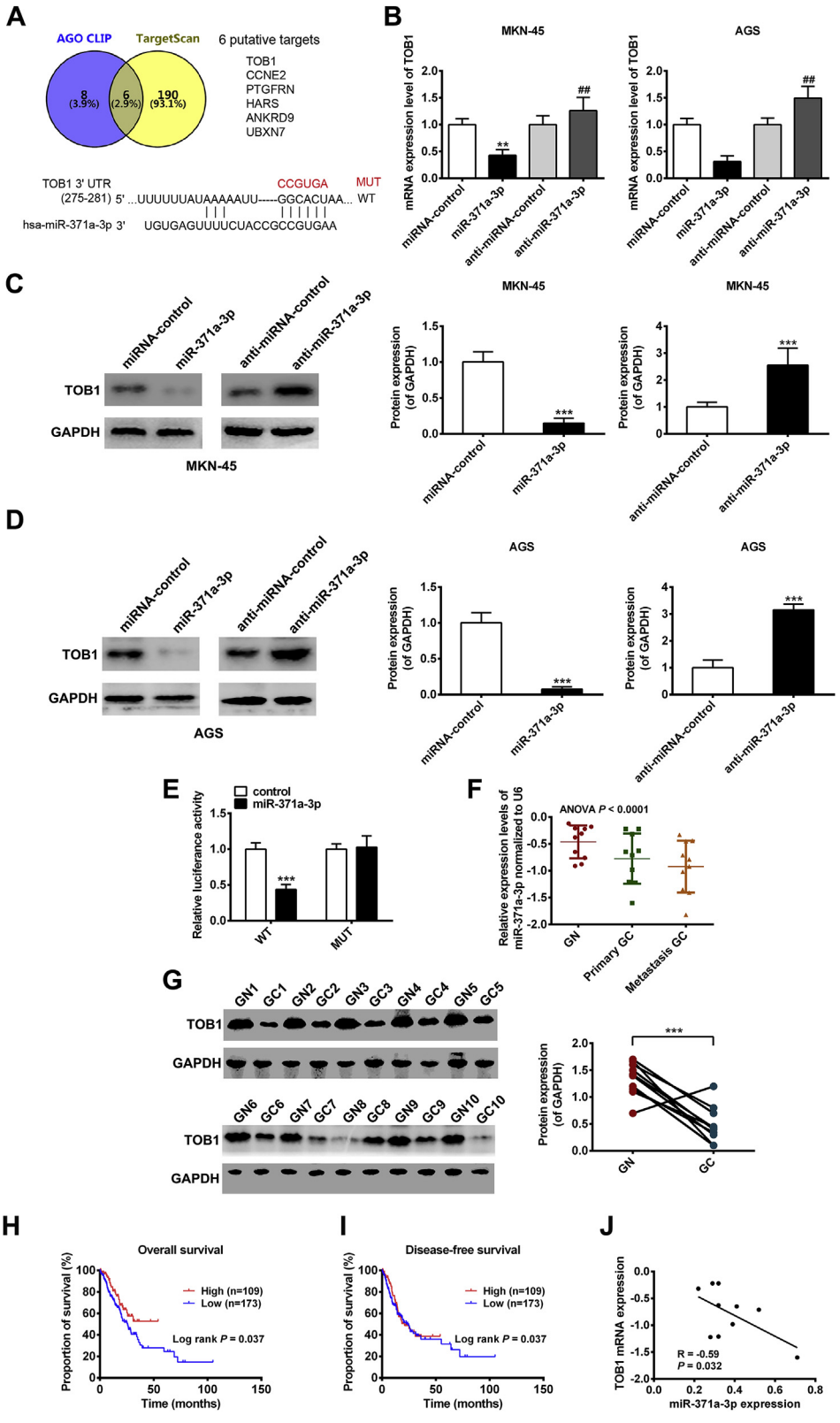

Fig. 4. miR-371a-3p suppresses TOB1 expression by directly binding to its 3'UTR. (**A**) Prediction of miR-371a-3p by two independent bioinformatics methods, TargetScan and AGO-CLIP sequencing from Starbase. (Top) Venn diagram showing predicted targets by each method. (Bottom) The sequence of miR-371a-3p binding sites within TOB1 3′ UTR. The reporter constructs containing wild-type TOB1 3′UTR sequences (WT) or the mutated 3′ UTR sequences (MUT) are shown, respectively. (**B**) Relative mRNA levels of TOB1 in MKN-45 (left) and AGS (right) cells upon miR-371a-3p mimics or inhibitor transfection. (**C-D**) Immunoblotting showing the protein levels of TOB1 in MKN-45 (left) and AGS (right) cells upon miR-371a-3p mimics or inhibitor transfection. (**E**) Luciferase reporter assays showing the relative luciferase activities of wide type (WT) and mutant (MUT) TOB1 reporters upon transfection of miR-371a-3p mimics. The luciferase reporter assays were conducted in HEK293T cells. (**F**) Relative mRNA levels of TOB1 in matched non-tumor tissues, primary GC tumors and metastasis tumors (n = 10)determined by qRT-PCR. P value was calculated by ANOVA test. (**G**) Immunoblotting showing the protein levels of TOB1 in paired GC tumors and non-tumor tissues (n = 10). (**H–I**) Kaplan-Meier curves indicate that the poor overall survival (**H**) and disease-free survival (**I**) of GC patients are positively associated with TOB1expression levels in TCGA samples. The GC patients were stratified into "high" and "low" groups by the average expression level of TOB1. (**J**) Correlation between miR-371a-3p levels and TOB1 mRNA levels in GC tumors (n = 10). The correlation was assessed by Pearson's correlation analysis. Student's *t* tests were performed. Data are presented as mean ± SD (*$P < 0.05$, **$P < 0.01$, ***$P < 0.001$).

Committee of the Affiliated Huaian No.1 People's Hospital of Nanjing Medical University and accorded with the Guidelines for the Care and Use of Laboratory Animals published by the National Institutes of Health.

2.9. Immunohistochemistry

Immunohistochemistry was performed using the following antibodies: anti-TOB1 (1:500, ab168947, Abcam, USA), anti-Ki-67 (1:500, ab16667, Abcam, USA) and anti-CD34 (1:500, ab81289, Abcam, USA) in xenograft tumors from the mouse model. The expression level was evaluated by integrating the percentage of positive cells and staining

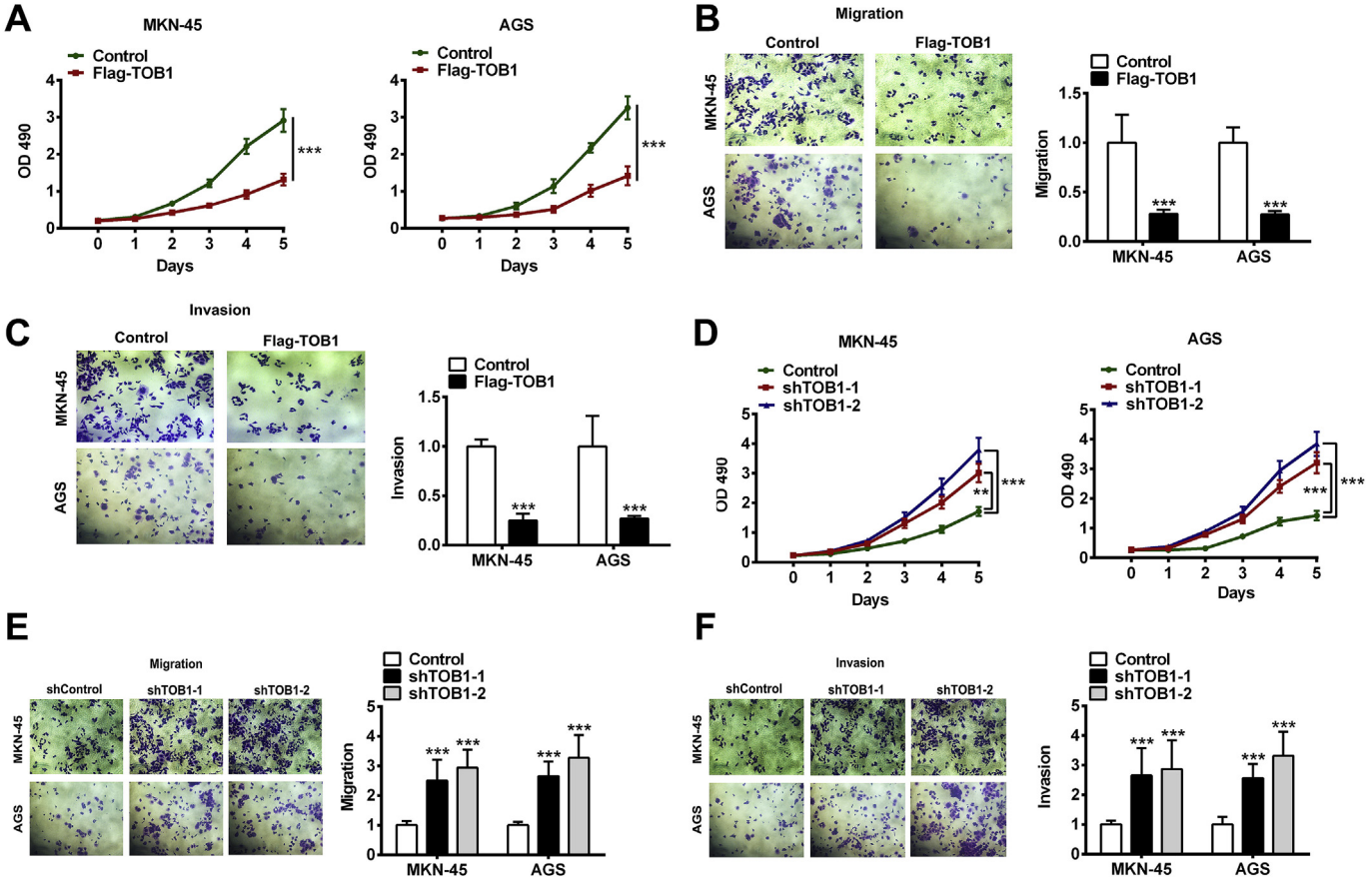

Fig. 5. TOB1 decreases GC cell proliferation, migration and invasion. (A–C) Effects of TOB1 overexpression on (A) cell proliferation by CCK8 assay, (B) cell migration (transwell assay), and (C) cell invasion (transwell assay) in AGS and MKN-45 cells. (D–F) Effects of shRNA-induced TOB1 inhibition on (D) cell proliferation by CCK8 assay, (E) cell migration (transwell assay), and (F) cell invasion (transwell assay) in AGS and MKN-45 cells. In CCK assays, cell proliferation was tested every 24 h. Student's *t* tests were performed. Data are presented as mean ± SD (*$P < 0.05$, ** $P < 0.01$, ***$P < 0.001$).

intensity. Staining intensity was scored as follows: negative (0), weak (1), moderate (2), and high (3). The extent of staining was scored according to the percentage of positive cells in the field: negative (0), 1%–10% (1), 11%–33% (2), 34%–66% (3), and 67%–100% (4). The percentage of positive cells and staining intensity scores were multiplied to calculate an immune-reactive score.

2.10. Statistical analysis

Each experiment was repeated at least three times. Data are presented as the mean values ± standard deviation (SD). The significance between groups was determined by two-tailed Student's *t*-test or the ANOVA test. The Kaplan-Meier method was used to estimate the survival rate and difference between the survival curves were assessed by log-rank test. The hazard ratio was calculated by univariate Cox proportional hazards regression. P values < 0.05 were considered statistically significant. Statistical analyses were performed by GraphPad Prism 5.0 software (GraphPad Software Inc., USA).

3. Results

3.1. Integrated analysis identified miR-371a-3p as a prognosis biomarker

Though numerous dysregulated miRNAs have been identified in GCs, the role and clinical significance have not been systematically investigated. Prognosis-associated miRNAs represent potential cancer markers that drive cell proliferation and migration during cancer progression in patients with poor survival. Thus, we performed an integrated analysis to identify potential prognosis-associated miRNAs in GCs. First, we explored the miRNA expression data in GC using The Cancer Genome Atlas (TCGA) project to identify dysregulated miRNAs in GC tumors compared to non-tumor tissues, which led to the discovery of a total of 74 miRNAs (Table S1). Then, these dysregulated miRNAs were subjected to survival analysis to assess the association between their expression level and the survival of GC patients. Results from the overall survival analyses showed that high levels of miR-135b-3p, miR-1306-3p, miR-196b-5p and miR-615-3p favored the outcomes in GC patients, whereas high levels of miR-371a-3p predicted shorter survival (Fig. 1A). In addition, disease-free survival analyses showed that increased levels of miR-509-3p, miR-3934-5p, miR-18a-3p and miR-508-3p were associated with longer survival, while high levels of miR-371a-3p and miR-449a were correlated with poor outcomes in GC patients (Fig. 1B). miR-196b-5p, miR-615-3p, miR-508-3p and miR-509-3p have all been identified as signature miRNAs in GCs [14–17]. Interestingly, among all the miRNAs identified, only miR-371a-3p was found to possess prognostic values for overall survival ($P = 0.01$; Fig. 1C) and disease-free survival ($P = 0.0034$; Fig. 1D). Furthermore, the up-regulation of miR-371a-3p in TCGA GC cohort (Fig. 1E) was further confirmed in another independent GC cohort (Fig. 1F).

3.2. miR-371a-3p expression is up-regulated in GCs and correlates with outcomes in patients

To further confirm the clinical findings, we performed qRT-PCR to investigate the miR-371a-3pexpression levels in 10 matched non-tumor tissues, primary GC tumors and metastatic tumors. Compared to non-tumor tissues, miR-371a-3p was significantly elevated in GC tumors (Fig. 2A). Additionally, our results showed a marked elevation of miR-

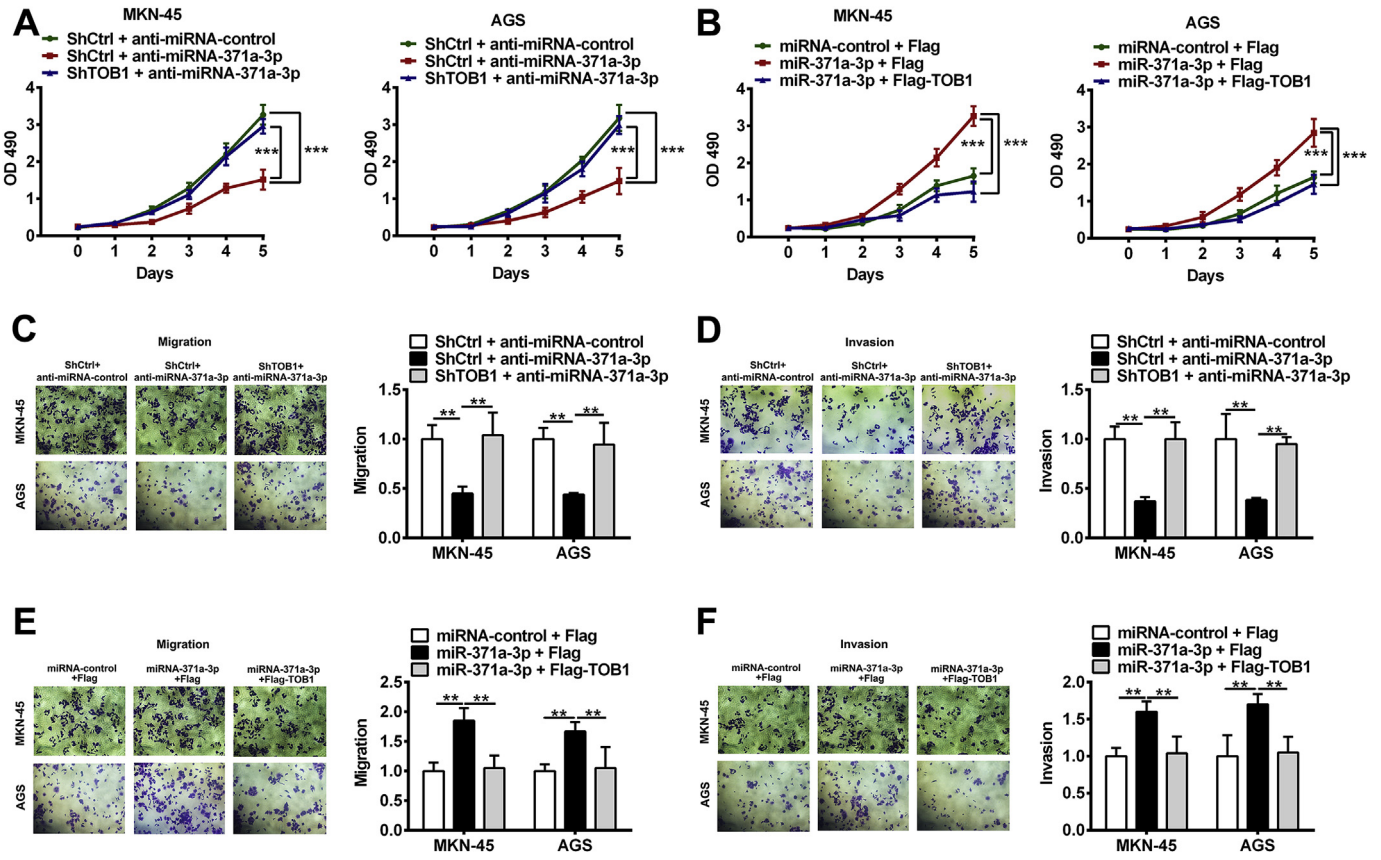

Fig. 6. miR-371a-3p functions are TOB1-dependent. (A–B) Assessment of cell proliferation by CCK assays in (A) TOB1-depeleted AGS and MKN-45 cells following transfection with miR-371a-3p inhibitor or scramble control, and (B) AGS and MKN-45 cells transfected with Flag-TOB1 plasmid or empty vector, along with miR-371a-3p mimics. Cell proliferation was tested every 24 h. (C–D) Measurement of cell migration by transwell assays in (C) TOB1-depeleted AGS and MKN-45 cells following transfection with miR-371a-3p inhibitor or scramble control, and (**D**) AGS and MKN-45 cells transfected with Flag-TOB1 plasmid or empty vector, along with miR-371a-3p mimics. (E–F) Cell invasion was evaluated by transwell assays in (E) TOB1-depeleted AGS and MKN-45 cells following transfection with miR-371a-3p inhibitor or scramble control, and (**F**) AGS and MKN-45 cells transfected with Flag-TOB1 plasmid or empty vector, along with miR-371a-3p mimics. Student's *t* tests were performed. Data are presented as mean ± SD (*$P < 0.05$, ** $P < 0.01$, ***$P < 0.001$).

371a-3p in the metastatic tumors compared to the primary tumors (Fig. 2A). Notably, the expression levels of miR-371a-3p were positively correlated with thickness of the gastric wall ($P < 0.0001$; Fig. 2B) and tumor stage at resection ($P < 0.0001$; Fig. 2C) in a total of 121 primary GC tumors. Consistent with the finding in TCGA cohort, GC patients with high expression of miR-371a-3p presented shorter survival (Fig. 2D). Altogether, our findings suggest that miR-371a-3p is a critical miRNA in the GC development and progression.

3.3. miR-371a-3p enhances GC cell proliferation, migration and invasion

To evaluate the functional effects of miR-371a-3pon GC cell proliferation, miR-371a-3p was overexpressed by transfecting miR-371a-3p mimics into GC cell lines, AGS and MKN-45. Results from the CCK-8 assays showed that up-regulation of miR-371a-3pmarkedly promoted the proliferative capability of GC cells (Fig. 3A). In line with this, we also observed that overexpression of miR-371a-3p greatly enhanced colony formation in AGS and MKN-45 cells (Fig. 3B). Then, we performed transwell assays to assess the involvement of miR-371a-3p in cell migration and invasion, which showed that up-regulation of miR-371a-3p also facilitated migration in AGS and MKN-45 cells (Fig. 3C). Consistently, the invasive capacity of AGS and MKN-45 cells was also enhanced by miR-371a-3p overexpression (Fig. 3D). These results indicate that miR-371a-3p overexpression promotes cell proliferation, migration and invasion.

Given the intriguing cell proliferation, migration and invasion promoting ability of miR-371a-3p, we sought to confirm whether inhibition of miR-371a-3p may result in opposite effects in GC cells. As expected, our results showed that miR-371a-3p inhibitor-induced downregulation of miR-371a-3p led to reduced cell proliferation, as shown in the CCK assay (Fig. 3E), decreased colony formation (Fig. 3F), and significant reduction in cell migration and invasion (Fig. 3G and H) in AGS and MKN-45 cells. Taken together, these results indicate that miR-371a-3p acts as an oncogenic modulator in GCs though promoting cell proliferation, migration and invasion.

3.4. miR-371a-3p directly targets TOB1

To further elucidate the underlying role and mechanism of miR-371a-3p in GC development and progression, we performed bioinformatics analyses to identify the functional targets of miR-371a-3p. By using the miRNA target prediction method TargetScan [18], we obtained a total of 196 putative targets of miR-371a-3p (Fig. 4A). To filter out the false positive candidates, we employed AGO-CLIP sequencing data from the StarBase [19], and identified 14 targets likely bound by miR-371a-3p (Fig. 4A). Finally, 6 target genes were predicted by both methods, among which TOB1 was ranked the first according to the number of supported AGO-CLIP datasets. miR-371a-3p has a binding site of 275–281 bp in the TOB1 3' UTR (Fig. 4A). Notably, previous studies have suggested TOB1 as a tumor suppressor that involves in cancer cell proliferation and migration [10–12]. Thus, the counteracting roles of miR-371a-3p and TOB1 in modulating cell malignant phenotypes prompted us to investigate the miRNA-target relationship between miR-371a-3p and TOB1.

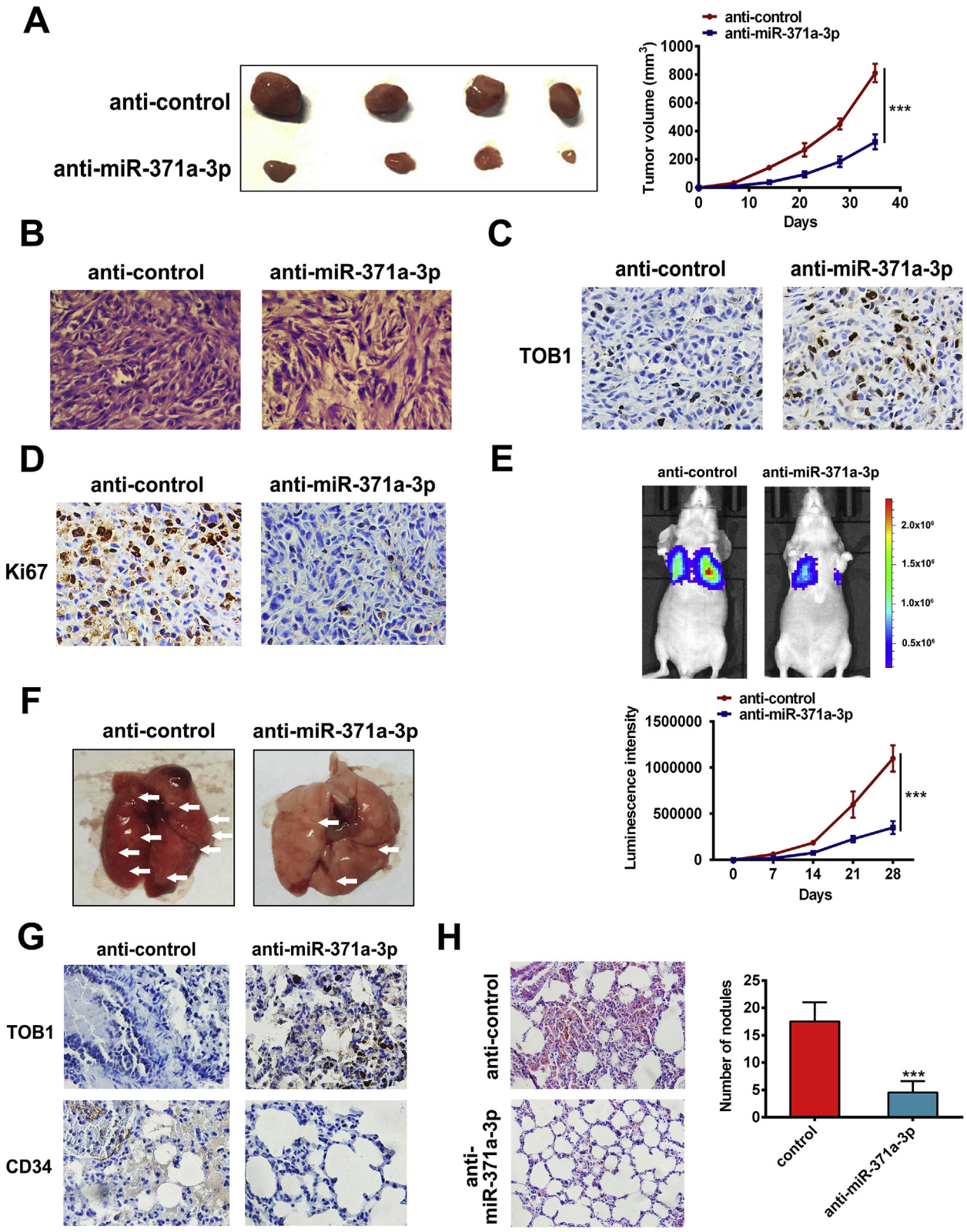

Fig. 7. Knockdown of miR-371a-3p inhibits GC cell growth and metastasis. (**A**) Tumor volume curves in xenograft formation assay by MKN-45 cells. MKN-45 cells transfected with control or miR-371a-3p antagomir were xenografted subcutaneously into the immunodeficient nude mice (n = 4 for each group). Left, representative images of xenograft tumors dissected from the nude mice. (**B**) Hematoxylin-eosin staining of xenograft tumors in (**A**). (**C-D**) Immunohistochemistry staining of xenograft tumors in (**A**) with anti-TOB1 (**C**) and anti-Ki-67 (**D**) antibodies. (**E**) Bioluminescence imaging curves of lung metastatic colonization by MKN-45 cells transfected with control or miR-371a-3p antagomir. The miR-371a-3p-depleted luciferase-tagged MKN-45 cells or control luciferase-tagged MKN-45 cells were injected into the tail vein of immunodeficient nude mice (n = 6 for each group). (**F**) Representative images of lungs excised from the mice in (**E**) and Hematoxylin-eosin staining (**G**). (**H**) Immunohistochemistry staining of tumors in (**F**) with anti-TOB1 and anti-CD34 antibodies. Student's *t* tests were performed. Data are presented as mean ± SD (*$P < 0.05$, ** $P < 0.01$, ***$P < 0.001$).

To test whether overexpression of miR-371a-3p affects TOB1 expression, the miR-371a-3p mimics were introduced into AGS and MKN-45 cells. The qRT-PCR assays showed that overexpression of miR-371a-3p suppressed the mRNA expression levels of TOB1 (Fig. 4B). On the contrary, when miR-371a-3p expression was inhibited by specific miR-371a-3p inhibitor, the mRNA expression levels of TOB1 were substantially elevated (Fig. 4B). This was further verified by western blotting, which consistently showed the decrease in the protein levels of TOB1 upon miR-371a-3p overexpression (Fig. 4C), and a marked increase in TOB1 levels following miR-371a-3p inhibition in MKN-45 cells (Fig. 4C). Similar results were observed in AGS cells (Fig. 4D).

To further investigate whether TOB1 is directly targeted by miR-371a-3p in GCs, luciferase assay was conducted using luciferase reporter plasmids, which contained either the wild-type (WT) or mutant (MUT) binding site of miR-371a-3p in the TOB1 3' UTR. The reporter vector (TOB1-WT or TOB1-MUT) and control or miR-371a-3p mimics were introduced into HEK-293T cells (Fig. 4E). Our results showed that cells expressing both miR-371a-3p mimics and TOB1-WT reporter exhibited a significant reduction in luciferase activities (Fig. 4E). On the contrary, no significant change was observed in the luciferase activities of TOB1-MUT reporter between miR-371a-3p and control groups (Fig. 4E). Additionally, the mRNA and protein levels of TOB1 were determined by qRT-PCR and immunoblotting, respectively, in the 10 paired GC tumors and non-tumor normal tissues. The levels of TOB1 were found to be significantly lower in GC tumors than non-tumor normal tissues at both mRNA and protein levels (Fig. 4F and G), implying that TOB1 may act as a tumor suppressor in GC. Of note, we also examined the prognosis value of TOB1 expression levels in GC patients and found that high level of TOB1 predicted better overall survival, but not disease-free survival (Fig. 4H and I). Furthermore, we examined the correlation between miR-371a-3p and TOB1 in GC tumors and observed a significant negative correlation between them ($R = -0.59$, $P = 0.032$; Fig. 4J). Taken together, these results indicate that TOB1 is a direct target of miR-371a-3p in GCs.

3.5. TOB1 decreases the abilities of GC cell proliferation, migration and invasion

Several studies have reported the function of TOB1 as a tumor suppressor in inhibiting cancer cell proliferation and migration [11,12]. However, TOB1 dysregulation has not been fully described in GC. In order to elucidate the role of TOB1 in GC, we then explored the effects of TOB1 on GC cell proliferation, migration and invasion. We transfected AGS and MKN-45 cells with Flag vector or Flag-TOB1, and observed the inhibition of proliferation, migration and invasion in AGS and MKN-45 cells following TOB1 up-regulation (Fig. 5A–C). In contrast, when TOB1 was knocked down by specific TOB1 shRNAs, cell proliferative, migratory and invasive abilities were substantially increased in AGS and MKN-45 cells (Fig. 5D–F). These results indicate that TOB1 plays a tumor-suppressing role in GCs.

3.6. The tumor-promoting role of miR-371a-3p is TOB1-dependent

To investigate whether miR-371a-3p tumor-promoting functions are dependent on TOB1, we first established stable TOB1-depletedAGS and MKN-45 cell lines by shRNAs. The TOB1-depeleted AGS and MKN-45 cells were treated with control or miR-371a-3p inhibitor. Our results showed that miR-371a-3p inhibition exerted anti-proliferative effects on GC cells without TOB1 depletion, but no effect was observed in TOB1-depleted AGS and MKN-45 cells (Fig. 6A). Additionally, we also performed rescue CCK-8 assays in AGS and MKN-45 cells to investigate whether re-expression of TOB1 can restore the pro-proliferation effects of miR-371a-3p on GC cells. miR-371a-3p was overexpressed in AGS and MKN-45 cells, and its effect was compared to restored TOB1. The result showed that miR-371a-3p overexpression could efficiently promote proliferation in GC cells (Fig. 6B). However, when TOB1 was restored in miR-371a-3p-overexpressing GC cells, the pro-proliferation effects were markedly eliminated in both AGS and MKN-45 cells (Fig. 6B).

Furthermore, we also assessed the requirement of TOB1 for miR-371a-3p's pro-migratory and pro-invasive abilities in GC cells. Consistent with the findings in CCK-8 assays, miR-371a-3p inhibition resulted in suppression of cell migration and invasion in AGS and MKN-45 cells without transfection of TOB1 shRNAs, but had no effect on cell migration and invasion in TOB1-depleted cells (Fig. 6C and E). The rescue assays also showed that overexpression of TOB1 reversed the promotion of GC cell migration and invasion caused by up-regulation of miR-371a-3p in AGS and MKN-45 cells (Fig. 6D and F). Collectively, these results indicate that TOB1 is the functional target of miR-371a-3p and is required for mediating the oncogenic effects of miR-371a-3p in promoting GC cell proliferation, migration and invasion.

3.7. Knockdown of miR-371a-3p inhibits GC growth and metastasis

The pivotal role of miR-371a-3p evidenced by *in vitro* experiments prompted us to confirm whether inhibition of miR-371a-3p could reduce GC cell growth and metastasis *in vivo*. We first conducted a subcutaneous mouse xenograft model to determine the role of miR-371a-3p depletion on GC cell growth *in vivo*. Stable miR-371a-3p-inhibiting and control MKN-45 cells were subcutaneously injected into each flank of immune-deficient nude mice and the tumor sizes were measured weekly for a period of 5 weeks. Our result showed that miR-371a-3p knockdown significantly inhibited tumor growth (Fig. 7A). Immunohistochemistry staining showed that TOB1 was markedly up-regulated in the xenograft tumors from miR-371a-3p-depleted group compared to controls (Fig. 7C), whereas the percentage of Ki-67-positive cells in miR-371a-3p-depleted tumors was much lower than controls, indicating a decrease in cell proliferation in MKN-45 cells caused by miR-371a-3p depletion (Fig. 7D). These results indicate strong inhibition of GC cell growth by miR-371a-3p *in vivo*.

Furthermore, we also conducted another mouse model experiment to confirm the metastasis-promoting role of miR-371a-3p *in vivo*. In brief, the luciferase-tagged MKN-45 cell line with stable miR-371a-3p knockdown was established. Then, the miR-371a-3p-depleted luciferase-tagged MKN-45 cells or control luciferase-tagged MKN-45 cells were injected into the tail vein of immune-deficient nude mice and lung metastases were monitored by BLI for four weeks. The result showed that inhibition of miR-371a-3p significantly suppressed GC cell metastasis (Fig. 7E). Hematoxylin-eosin staining of the lungs showed more tumor nodules in the lungs from the miR-371a-3p-depleted mice than that in controls (Fig. 7G). Notably, the immunohistochemistry staining also showed the upregulation of TOB1 but marked decrease in CD34 in miR-371a-3p-depleted tumors, indicating the anti-angiogenic of miR-371a-3p depletion (Fig. 7H). Taken together, our results indicate that miR-371a-3p plays a critical role in control of GC cell metastasis *in vivo*.

4. Discussion

Despite numerous study describing miRNAs in GCs, the clinical significance and underlying mechanism of miRNAs in GCs have not been systematically investigated. In the present study, we have identified a GC-critical miRNA, miR-371a-3p through integrated analyses. We show that miR-371a-3p was elevated in GC tumors compared to non-tumor normal tissues, suggesting the potential use of miR-371a-3p as a biomarker for GC prognosis. Further *in vitro* and *in vivo* functional assays demonstrated that miR-371a-3p promoted GC cell growth and metastasis through directly targeting TOB1, a tumor suppressor gene. We here for the first time establish the oncogenic role of miR-371a-3p in GC, providing a promising target for the treatment of GCs.

miR-371a-3p is located at chromosome 19q13.4. Recent studies have implicated 19q13.4 genomic aberrations in benign thyroid tumors. Targeting the miRNA clusters, C19MC and miR-371-3, which

leads to their transcriptional activation, is likely due to juxtaposing them to transcriptional activators [20] or by depletion of CpG islands upstream of the clusters [21]. Overexpression of the miR-371a-3pmiRNA clusters has been found to increase invasive activities in cancer cells [22,23]. Additionally, a recent study provides evidence that miR-371a-3p serum levels are likely to be a useful biomarker for detection of germ cell tumors [24]. However, the biological function of miR-371a-3premains poorly understood. Our study show that miR-371a-3p was up-regulated in GC tumors and it can promote GC cell growth and metastasis *in vitro* and *in vivo*. The current study was carried out in an immunodeficient mouse model, which warrants a further study to confirm the role of miR-371a-3p in GC development and progression.

In this study, we establish TOB1 as a functional downstream target of miR-371a-3p.TOB1 is a well-known tumor suppressor, which has been found to be inactivated in many types of cancers, including GC. Previous studies have shown that TOB1 overexpression inhibits proliferation, migration and invasion in GC cells while promoting GC cell apoptosis through enhancing Smad4 and decreasing β-catenin signaling activities [25]. TOB1 has also been found to be a downstream effector of EGF signaling through inducing phosphorylation of HER2 [26]. Our study shows that TOB1 acts as a tumor suppressor that inhibits GC cell proliferation and migration. Like many other tumor suppressors, TOB1 is frequently decreased in various cancers. Previous studies have indicated that TOB1 was either absent or present at low levels in 75% of GCs [27]. However, the mechanism underlying the loss of TOB1 has not been illustrated. In the present study, we show that the absence of TOB1 in GCs was mainly modulated by miR-371a-3p overexpression, although we cannot exclude the possibility that TOB1 may also be regulated by other mechanisms, such as loss-of-function mutation, copy number depletion or hyper-methylation.

5. Conclusion

In summary, we reveal the upregulation of miR-371a-3pin GCs, proving it to be a potential prognosis biomarker for GC through integrated analyses. Functional assays demonstrate that miR-371a-3p promotes GC cell growth and metastasis *in vitro* and *in vivo*. Additionally, we identify TOB1 as a direct target ofmiR-371a-3p, and is essential for mediating the oncogenic effects of miR-371a-3p in GC cells. Therefore, this study demonstrates that targeting miR-371a-3p-TOB1 axis may be a potential novel strategy for GC treatment.

Conflicts of interest

The authors declare that there is no conflict of interest associated with this work.

Acknowledgement

This work was funded as part of a project titled ‘To observe the clinical effect of Xiao'ai Jiedu decoction combined with radiotherapy in treatment of esophageal carcinoma and the effect on MicroRNAs’ (grant no. LZ13180).

Appendix A. Supplementary data

Supplementary data to this article can be found online at https://doi.org/10.1016/j.canlet.2018.11.021.

References

[1] J. Ferlay, E. Steliarova-Foucher, J. Lortet-Tieulent, S. Rosso, J.W. Coebergh, H. Comber, D. Forman, F. Bray, Cancer incidence and mortality patterns in Europe: estimates for 40 countries in 2012, Eur. J. Canc. 49 (2013) 1374–1403.
[2] W. Yasui, K. Sentani, N. Sakamoto, K. Anami, Y. Naito, N. Oue, Molecular pathology of gastric cancer: research and practice, Pathol. Res. Pract. 207 (2011) 608–612.
[3] D.P. Bartel, MicroRNAs: target recognition and regulatory functions, Cell 136 (2009) 215–233.
[4] D.P. Bartel, MicroRNAs: genomics, biogenesis, mechanism, and function, Cell 116 (2004) 281–297.
[5] Q. Ji, X. Hao, Y. Meng, M. Zhang, J. Desano, D. Fan, L. Xu, Restoration of tumor suppressor miR-34 inhibits human p53-mutant gastric cancer tumorspheres, BMC Canc. 8 (2008) 266.
[6] Z. Wang, X. Ma, Q. Cai, X. Wang, B. Yu, Q. Cai, B. liu, Z. Zhu, C. Li, MiR-199a-3p promotes gastric cancer progression by targeting ZHX1, FEBS Lett. 588 (2014) 4504–4512.
[7] N. Nishida, K. Mimori, M. Fabbri, T. Yokobori, T. Sudo, F. Tanaka, K. Shibata, H. Ishii, Y. Doki, M. Mori, MicroRNA-125a-5p is an independent prognostic factor in gastric cancer and inhibits the proliferation of human gastric cancer cells in combination with trastuzumab, Clin. Canc. Res. : Off. J. Am. Asso. Canc. Res. 17 (2011) 2725–2733.
[8] B. Zheng, L. Liang, C. Wang, S. Huang, X. Cao, R. Zha, L. Liu, D. Jia, Q. Tian, J. Wu, Y. Ye, Q. Wang, Z. Long, Y. Zhou, C. Du, X. He, Y. Shi, MicroRNA-148a suppresses tumor cell invasion and metastasis by downregulating ROCK1 in gastric cancer, Clinical cancer research, Off. J. Am. Asso. Canc. Res. 17 (2011) 7574–7583.
[9] F. Guehenneux, L. Duret, M.B. Callanan, R. Bouhas, S. Hayette, C. Berthet, C. Samarut, R. Rimokh, A.M. Birot, Q. Wang, J.P. Magaud, J.P. Rouault, Cloning of the mouse BTG3 gene and definition of a new gene family (the BTG family) involved in the negative control of the cell cycle, Leukemia 11 (1997) 370–375.
[10] R. Guan, L. Peng, D. Wang, H. He, D. Wang, R. Zhang, H. Wang, H. Hao, J. Zhang, H. Song, S. Sui, X. Meng, X. Cui, J. Bai, W. Sun, S. Fu, J. Yu, Decreased TOB1 expression and increased phosphorylation of nuclear TOB1 promotes gastric cancer, Oncotarget 8 (2017) 75243–75253.
[11] D. Wu, W. Zhou, S. Wang, Z. Zhou, S. Wang, L. Chen, Tob1 enhances radiosensitivity of breast cancer cells involving the JNK and p38 pathways, Cell Biol. Int. 39 (2015) 1425–1430.
[12] Y.W. Zhang, R.E. Nasto, R. Varghese, S.A. Jablonski, I.G. Serebriiskii, R. Surana, V.S. Calvert, I. Bebu, J. Murray, L. Jin, M. Johnson, R. Riggins, H. Ressom, E. Petricoin, R. Clarke, E.A. Golemis, L.M. Weiner, Acquisition of estrogen independence induces TOB1-related mechanisms supporting breast cancer cell proliferation, Oncogene 35 (2016) 1643–1656.
[13] J. Zhou, J. Zhou, W. Wang, W. Li, L. Wu, G. Li, J. Shi, S. Zhou, The polymorphism in miR-25 attenuated the oncogenic function in gastric cancer, Tumour biol.: J. Int. Soc. Oncodev. Biol. Med. 37 (2016) 5515–5520.
[14] J.Y. Lim, S.O. Yoon, S.Y. Seol, S.W. Hong, J.W. Kim, S.H. Choi, J.S. Lee, J.Y. Cho, Overexpression of miR-196b and HOXA10 characterize a poor-prognosis gastric cancer subtype, World J. Gastroenterol. 19 (2013) 7078–7088.
[15] J. Wang, L. Liu, Y. Sun, Y. Xue, J. Qu, S. Pan, H. Li, H. Qu, J. Wang, J. Zhanga, miR-615-3p promotes proliferation and migration and inhibits apoptosis through its potential target CELF2 in gastric cancer, Biomed. Pharmacother. Biomed. Pharmacother. 101 (2018) 406–413.
[16] J. Sun, J. Li, W. Zhang, J. Zhang, S. Sun, G. Li, H. Song, D. Wan, MicroRNA-509-3p inhibits cancer cell proliferation and migration via upregulation of XIAP in gastric cancer cells, Oncol. Res. 25 (2017) 455–461.
[17] T. Huang, W. Kang, B. Zhang, F. Wu, Y. Dong, J.H. Tong, W. Yang, Y. Zhou, L. Zhang, A.S. Cheng, J. Yu, K.F. To, miR-508-3p concordantly silences NFKB1 and RELA to inactivate canonical NF-kappaB signaling in gastric carcinogenesis, Mol. Canc. 15 (2016) 9.
[18] V. Agarwal, G.W. Bell, J.W. Nam, D.P. Bartel, Predicting effective microRNA target sites in mammalian mRNAs, eLife (2015) 4.
[19] J.H. Yang, J.H. Li, P. Shao, H. Zhou, Y.Q. Chen, L.H. Qu, starBase: a database for exploring microRNA-mRNA interaction maps from Argonaute CLIP-Seq and Degradome-Seq data, Nucleic Acids Res. 39 (2011) D202–D209.
[20] V. Rippe, L. Dittberner, V.N. Lorenz, N. Drieschner, R. Nimzyk, W. Sendt, K. Junker, G. Belge, J. Bullerdiek, The two stem cell microRNA gene clusters C19MC and miR-371-3 are activated by specific chromosomal rearrangements in a subgroup of thyroid adenomas, PLoS One 5 (2010) e9485.
[21] K.W. Tsai, H.W. Kao, H.C. Chen, S.J. Chen, W.C. Lin, Epigenetic control of the expression of a primate-specific microRNA cluster in human cancer cells, Epigenetics 4 (2009) 587–592.
[22] Q. Huang, K. Gumireddy, M. Schrier, C. le Sage, R. Nagel, S. Nair, D.A. Egan, A. Li, G. Huang, A.J. Klein-Szanto, P.A. Gimotty, D. Katsaros, G. Coukos, L. Zhang, E. Pure, R. Agami, The microRNAs miR-373 and miR-520c promote tumour invasion and metastasis, Nat. Cell Biol. 10 (2008) 202–210.
[23] S. Cairo, Y. Wang, A. de Reynies, K. Duroure, J. Dahan, M.J. Redon, M. Fabre, M. McClelland, X.W. Wang, C.M. Croce, M.A. Buendia, Stem cell-like micro-RNA signature driven by Myc in aggressive liver cancer, Proc. Natl. Acad. Sci. U. S. A 107 (2010) 20471–20476.
[24] K.P. Dieckmann, M. Spiekermann, T. Balks, I. Flor, T. Loning, J. Bullerdiek, G. Belge, MicroRNAs miR-371-3 in serum as diagnostic tools in the management of testicular germ cell tumours, Br. J. Canc. 107 (2012) 1754–1760.
[25] J. Kundu, S.M. Wahab, J.K. Kundu, Y.L. Choi, O.C. Erkin, H.S. Lee, S.G. Park, Y.K. Shin, Tob1 induces apoptosis and inhibits proliferation, migration and invasion of gastric cancer cells by activating Smad4 and inhibiting betacatenin signaling, Int. J. Oncol. 41 (2012) 839–848.
[26] M.W. Helms, D. Kemming, C.H. Contag, H. Pospisil, K. Bartkowiak, A. Wang, S.Y. Chang, H. Buerger, B.H. Brandt, TOB1 is regulated by EGF-dependent HER2 and EGFR signaling, is highly phosphorylated, and indicates poor prognosis in node-negative breast cancer, Cancer Res. 69 (2009) 5049–5056.
[27] J. Yu, P. Liu, X. Cui, Y. Sui, G. Ji, R. Guan, D. Sun, W. Ji, F. Liu, A. Liu, Y. Zhao, Y. Yu, Y. Jin, J. Bai, J. Geng, Y. Xue, J. Qi, K.Y. Lee, S. Fu, Identification of novel subregions of LOH in gastric cancer and analysis of the HIC1 and TOB1 tumor suppressor genes in these subregions, Mol. Cell. 32 (2011) 47–55.